PERGAMON

International Journal of Heat and Mass Transfer 43 (2000) 2793–2806

International Journal of HEAT and MASS TRANSFER

www.elsevier.com/locate/ijhmt

Sublimation and vaporization of an ice aerosol particle in the form of thin cylinder by laser radiation

A.N. Kucherov

Department of Fundamental Research, Central Aerohydrodynamic Institute (TsAGI), 140160 Zhukovsky, Moscow, Russia

Received 17 September 1998

Abstract

Formulae for heat and mass exchange from the surface of ice particles of different forms are derived. Destruction of plate, cylindrical and spherical particles in the sublimation regime, as well as the subsequent melting (cylinder, disk) and evaporation of the water droplet formed are investigated. The study was conducted for the parameters averaged over the particle volume: heat release intensity, temperature, evaporation efficiency, etc. Heating time, melting time, evaporation time, evaporation efficiency, temperature for particles in the form of thin long cylinder is presented versus the intensity of laser radiation at various temperatures and pressures of the surrounding air. The results are compared with the correspondent evaporation parameters of a supercooled spherical water droplet. © 2000 Elsevier Science Ltd. All rights reserved.

1. Introduction

When we investigate clearing of a water aerosol (mist, clouds, aircraft condensation trail) by the laser radiation including the solid phase, a study of interaction between radiation and a single particle is a necessary stage. Usually three groups of particles are distinguished: plates, cylinders, spheres [1–3]. The question of temperature and other conditions of aerosol particles freezing is not completely cleared. There is evidence for existence of supercooled droplets at a temperature of -40°C (233 K) [4,5]. If some acid (nitric, sulphuric, etc.) is present in droplets, the liquid phase can exist at a temperature over 200 K [6]. Evaporation of a spherical water droplet is well investigated [7–9]. Evaporation of ice crystals is not practically investigated. Some experimental and theoretical data on the evaporation of ice plates are presented in [10–13]. In the present work, sublimation and evaporation of ice aerosol particles in the form of long thin cylinder is investigated. The results are compared with the evaporation characteristics of plate ice disk and supercooled spherical water droplet.

2. Mass and heat fluxes from the particle surface

Let us derive general formulae for heat and mass exchange with the surrounding air. We shall consider an ice aerosol particle having the form of a flat disk of radius $L \gg a$ (where $a = h/2$, is half-thickness of the disk), a cylinder of radius a and length $L \ll a$ or a sphere of radius a. The mass and energy conservation equations, the equation of vapor diffusion through air, the air and vapor state equations have the following form [14]:

E-mail address: ank@dept.aerocentr.msk.su (A.N. Kucherov).

0017-9310/00/$ - see front matter © 2000 Elsevier Science Ltd. All rights reserved.
PII: S0017-9310(99)00321-X

Nomenclature

a	small size of particle (half-thickness of plate and radius of cylinder)
b	evaporation efficiency
C_p	specific heat at constant pressure
D	diffusion coefficient
H	the specific heat of water evaporation H_w or ice sublimation H_i
I	radiation intensity
j	density of the vapor mass flow
j_T	density of energy flow
L	big size of particle (radius of disk and length of cylinder)
p	pressure
q	heat release intensity
T	temperature
u, v	velocities
Y	mass concentration of the vapour and air in the mixture

Greek symbols

α	absorption coefficient
β	evaporation parameter
λ	coefficient of the heat conductivity of air–vapor mixture
μ	molar mass
ρ	density

Subscripts

a	air
av	averaged
i	ice
s	surface of the particle
w	water

$$\frac{\partial \rho_v}{\partial t} + \operatorname{div}\left[\rho_v(\vec{u}+\vec{v}_v)\right] = 0;$$
$$\frac{\partial \rho_a}{\partial t} + \operatorname{div}\left[\rho_a(\vec{u}+\vec{v}_a)\right] = 0; \quad \frac{\partial \rho}{\partial t} + \operatorname{div}\left[\rho\vec{u}\right] = 0 \tag{1}$$

$$\frac{\partial}{\partial t}\left[\rho\left(C_pT + \frac{u^2}{2}\right)\right] - \frac{\partial p}{\partial t} + \operatorname{div}\left[\rho\vec{u}\left(C_pT + \frac{u^2}{2}\right) - \lambda \operatorname{grad} T\right] = 0; \quad T|_{r=a} = T_s; \quad T|_{r\to\infty} \to T_\infty \tag{2}$$

$$-Y_v\vec{v}_v = Y_a\vec{v}_a = D\vec{\nabla}Y_v;$$
$$Y_v|_{r=a} = Y_{vs}; \quad Y_v|_{r\to\infty} \to Y_\infty$$
$$Y_v = \frac{\rho_v}{\rho} = \frac{\mu_v p_v}{\mu p}; \quad Y_a = \frac{\rho_a}{\rho}; \quad Y_v + Y_a = 1; \tag{3}$$
$$\rho = \rho_v + \rho_a; \quad p = p_a + p_v; \quad \frac{1}{\mu} = \frac{Y_v}{\mu_v} + \frac{Y_a}{\mu_a}$$

$$p = \rho\frac{R}{\mu}T; \quad p_v = \rho_v\frac{R}{\mu_v}T; \quad p_a = \rho_a\frac{R}{\mu_a}T \tag{4}$$

$$p_{sv} = p_1 \exp\left\{\int_{T_1}^{T_s} \frac{\mu_v H(T)\,dT}{RT^2}\right\} \tag{5}$$

Here ρ, ρ_v, ρ_a, p, p_v, p_a, u, v_v, v_a are densities, pressures and velocities of mixture, vapor and air; C_p, λ, D are specific heat and mixture coefficients of the heat conductivity and diffusion; μ, μ_v, μ_a are molar masses of the mixture, vapour and air; Y_v, Y_a are mass concentrations of the vapour and air in the mixture, Y_∞ is vapor concentration at infinity; T_s, T_∞ are temperatures on the surface of the particle and the gas at infinity; H is the specific heat of water evaporation H_w or ice sublimation H_i; p_1 is the known value of saturation pressure at a temperature of T_1 ($p_1 = 1$ bar at $T_1 = 373$ K). The Clausius–Clapeyron equation (5) relates the saturated vapor pressure p_{sv} with the surface temperature T_s. We neglected the viscosity members in the equation of energy conservation (2), barodiffusion and thermal diffusion in Eq. (3). Since the vapor and air density is by a factor of 10^3 less than water and ice density, the characteristic times of heat and mass transfer in the gas are by several orders of magnitude less. Heat and mass transfer outside the particle is quasi-stationary. The gas flow is one-dimensional for a disk everywhere, excluding the close vicinity of edges and axisymmetrical for a cylinder far from its ends. The stationary equations of mass conservation (1) have the following integrals for the cases of plane, cylindrical and spherical symmetry:

$$r^m\rho_v(u+v_v) = a^m j; \quad r^m\rho_a(u+v_a) = 0;$$
$$r^m\rho u = a^m j \tag{6}$$

Here $m = 0$, 1, 2 for the plate, cylinder and sphere, j is density of the vapor flow from the particle surface.

The stationary equation (2) has the following first integral:

$$r^m\left[\rho u\left(C_p T+\frac{u^2}{2}\right)-\lambda\frac{\partial T}{\partial r}\right]=a^m j_T \tag{7}$$

At a slow heating rate and a surface temperature T_s less than the boiling temperature T_b, it is possible to neglect the vapor kinetic energy $u^2/2$. At $T_s > T_b$, it is possible to neglect the ambient medium heat conduction (member $-\lambda\partial T/\partial r$). The value j_T is density of energy flow from the particle surface. We shall take the specific heat capacity of mixture C_p, the thermal conductivity λ and the product ρD of the mixture density ρ by the vapor diffusivity D as constant and equal to some average (over the temperature) values. Replacing the velocity using Eq. (6) from Eqs. (3) and (7), and taking into account particle surface boundary conditions, we get expressions for gas temperature and mass concentrations of the vapor outside the plate (disk), cylinder and sphere:

$$T(r)=\begin{cases}\left(T_s-\dfrac{j_T}{jC_p}\right)\mathrm{e}^{\,jC_p(r-a)/\lambda}+\dfrac{j_T}{jC_p}, & m=0\\ \left(T_s-\dfrac{j_T}{jC_p}\right)\left(\dfrac{r}{a}\right)^{jC_p a/\lambda}+\dfrac{j_T}{jC_p}, & m=1\\ \left(T_s-\dfrac{j_T}{jC_p}\right)\mathrm{e}^{\,jC_p a(1-a/r)/\lambda}+\dfrac{j_T}{jC_p}, & m=2\end{cases};$$

$$Y_v(r)=\begin{cases}1-(1-Y_{vs})\,\mathrm{e}^{\,j(r-a)/\rho D}, & m=0\\ 1-(1-Y_{vs})\left(\dfrac{r}{a}\right)^{ja/\rho D}, & m=1\\ 1-(1-Y_{vs})\,\mathrm{e}^{\,ja(1-a/r)/\rho D}, & m=2\end{cases} \tag{8}$$

In case of a sphere ($m=2$) using conditions at infinity, we find the following expressions for the flows of mass and heat from the droplet surface:

$$j=\frac{\rho D}{a}\ln\left(\frac{1-Y_\infty}{1-Y_{vs}}\right);$$

$$j_T=jC_p\frac{T_s\exp\left(jC_p a/\lambda\right)-T_\infty}{\exp\left(jC_p a/\lambda\right)-1} \tag{9}$$

For $Y_v < 1$, it is possible to take the pressure of mixture approximately equal to the pressure at infinity. Expressions (9) give boundary conditions $j(T_s)$, $j_T(T_s)$ for a spherical droplet.

In the cases of a cylinder or a plate, the solutions (8) unlimitedly decrease at great distances, which disagree with the physical sense. Let us build auxiliary solutions $Y_v(r)$, $T(r)$ in the field of great $r \geq L$ and conjugate these external solutions with the internal one (8). At $r \gg L$, the flow may be considered as spherically symmetrical. Let us introduce in Eqs. (6) and (7) the flow density of mass j_L and heat j_{TL} at a sphere of the radius $r_L = AL$. Here A is a constant that may be found by comparing the results with a rigorous numerical solution or with experimental data. Conservation of mass and heat flows through the surfaces of a disk or a cylinder, on the one hand, and a sphere of the radius r_L, on the other, gives simple relationships for

$$\begin{aligned}&\text{disk } (m=0): \quad j_L\approx\frac{j}{2A^2};\ j_{TL}\approx\frac{j_T}{2A^2};\\ &\text{and cylinder } (m=1): \quad j_L\approx\frac{ja}{2A^2L};\ j_{TL}\approx\frac{j_T a}{2A^2L}.\end{aligned} \tag{10}$$

Instead of the surface conditions for functions $Y_v(r)$ and $T(r)$, we use the conditions at great $r\to\infty$. Then the solutions similar to Eq. (8) will be written as:

$$\begin{aligned}&T(r)=\left(T_\infty-\frac{j_{TL}}{j_L C_p}\right)\mathrm{e}^{-jC_p A^2L^2/\lambda r}+\frac{j_{TL}}{j_L C_p};\\ &Y(r)=1-(1-Y_\infty)\,\mathrm{e}^{-jA^2L^2/\rho Dr}\end{aligned} \tag{11}$$

At coordinate $r = r_L$, we will equate solutions (8) and (11). Then, we will get implicit dependence of the flows of mass j and heat j_T at the particle surfaces on the surface temperature T_s:

$$j=\frac{\rho D}{r_{ef}}\ln\left(\frac{1-Y_\infty}{1-Y_{vs}}\right);$$

$$j_T=jC_p\frac{T_s\exp\left(jC_p r_{ef}/\lambda\right)-T_\infty}{\exp\left(jC_p r_{ef}/\lambda\right)-1}$$

$$r_{ef}=\begin{cases}L\left(A+1/2A+a/A^3L\right)-a, & m=0\\ a\left[\ln(AL/a)+(1+a/L)/2A\right], & m=1\\ a, & m=2\end{cases}. \tag{12}$$

Expressions (12) give boundary conditions of heat and mass transfer on the surface of the vaporized particles having the form of disk ($m=0$), cylinder ($m=1$), sphere ($m=2$) for *diffusive* and *diffusive–convective* regimes of evaporation. The three classes of particles are distinguished by the effective radius r_{ef}. At high intensities of heat release and surface temperature exceeding the water boiling temperature ($T_s > T_b$), vapour displaces air. *Subsonic* and *sonic* regimes of evaporation are realized, in which values j, j_T are independent of the geometric form and size and only depend on the surface temperature T_s.

3. Heat sources inside particles

Inside a particle (disk, cylinder, sphere), the process of heating is described by the heat conduction equation for ice and the boundary condition for mass sublimation from the surface:

$$\rho_{\mathrm{i}} C_{\mathrm{pi}} \frac{\partial T}{\partial t} = \frac{1}{r^m} \frac{\partial}{\partial r}\left(r^m \lambda_{\mathrm{i}} \frac{\partial T}{\partial r} \right) + q;$$
$$T(r, t=0) = T_\infty; \quad \mp \lambda_{\mathrm{i}} \left.\frac{\partial T}{\partial r}\right|_{r=0;\, h;\, a} = jH_{\mathrm{i}} + j_T \tag{13}$$

$$\frac{\mathrm{d}a}{\mathrm{d}t} = -\frac{j}{\rho_{\mathrm{i}}}; \quad a|_{t=0} = a_0 \tag{14}$$

Subscript "i" denotes ice; $q = \alpha I_0$ is the heat release intensity averaged over volume, α is the average absorption coefficient, I_0 is the characteristic intensity of radiation. By definition:

$$q = \frac{W_{\mathrm{abs}}}{V} = \frac{\int \alpha_{\mathrm{i,\,w}} I \,\mathrm{d}V}{V} = \alpha I_0,$$
$$Q_{\mathrm{abs}} = \frac{W_{\mathrm{abs}}}{G I_0} = \frac{\alpha V}{G} \tag{15}$$

Here W_{abs} is the energy absorbed per unit of time in the volume of a particle V ($V = 2a\pi L^2$; $\pi a^2 L$; $4\pi a^3/3$ for the disk, cylinder and sphere, respectively), $\alpha_{\mathrm{i,\,w}} = 4\pi\kappa_{\mathrm{i,\,w}}/\lambda$ is the coefficient of radiation absorption with a wavelength λ in the medium with the absorption index equal to $\kappa_{\mathrm{i,\,w}}$ (i: ice, w: water); Q_{abs} is a factor of radiation absorption on a single particle; $G = \pi L^2 (m=0)$; $2aL (m=1)$; $\pi a^2 (m=2)$ is an area of particle section by a plane perpendicular to the axis of the laser beam. In the case of the oblique incidence of beam at angle $\theta_1 > a/L$ (with the local vertical on the plane of the disk or with the axis of the cylinder), the flow of radiation energy W and the section area of particle G are:

$$W = I_0 \pi L^2 \cos\theta_1, m=0; \quad I_0 2aL \cos\theta_1, m=1;$$
$$I_0 \pi a^2, m=2$$
$$G = \pi L^2 \cos\theta_1; \quad 2aL\cos\theta_1; \quad \pi a^2$$

Let us take a look at radiation wavelength $\lambda = 10.6$ μm in the following optical constants of ice and water: $n_{\mathrm{i}} = 1.195$; $\kappa_{\mathrm{i}} = 0.0690$; $\alpha_{\mathrm{i}} = 7.14 \times 10^4$ m^{-1}; $n_{\mathrm{w}} = 1.185$; $\kappa_{\mathrm{w}} = 0.0602$; $\alpha_{\mathrm{w}} = 8.18 \times 10^4$ m^{-1} [15].

For a flat disk of thickness $h = 2a$ and radius $L \gg a$, using the expressions for the coefficient of reflection R and the coefficient of transmission T for an unlimited plate of thickness h [16], we get:

$$W_{\mathrm{abs}} = (1 - R - T) W;$$
$$\alpha = \frac{W_{\mathrm{abs}}}{V I_0} = (1 - R - T)\frac{\cos\theta_1}{2a}; \quad Q_{\mathrm{abs}} = \frac{W_{\mathrm{abs}}}{G I_0} = (1 - R - T) \tag{16}$$

$$R = \frac{|r_\perp|^2 + |r_\parallel|^2}{2}; \quad r = \frac{r_{12} + r_{23}\,\mathrm{e}^{2i\beta}}{1 + r_{12} r_{23}\,\mathrm{e}^{2i\beta}};$$
$$T = \frac{|t_\perp|^2 + |t_\parallel|^2}{2}; \quad t = \frac{t_{12} t_{23}\,\mathrm{e}^{i\beta}}{1 + r_{12} r_{23}\,\mathrm{e}^{2i\beta}} \tag{17}$$

$$r_{12} = \frac{p_1 - p_2}{p_1 + p_2}; \quad r_{23} = \frac{p_2 - p_3}{p_2 + p_3}; \quad t_{12} = \frac{2p_1}{p_1 + p_2};$$
$$t_{23} = \frac{2p_2}{p_2 + p_3}$$

$$(p_j)_\perp = n_j \cos\theta_j; \quad (p_j)_\parallel = n_j^{-1} \cos\theta_j; \quad j = 1, 2, 3;$$
$$\beta = \frac{2\pi}{\lambda} n_2 h \cos\theta_2; \; n_1 \sin\theta_1 = n_2 \sin\theta_2;$$
$$n_2 \sin\theta_2 = n_3 \sin\theta_3$$

Here 1, 3 denote the surrounding medium (air), 2 denotes the matter of the plate (ice).

Expressions for the extinction factor Q_{ext}, scattering factor Q_{sca} and absorption factor Q_{abs} for an unlimited cylinder or sphere are presented in [3] together with programs for calculation of these factors (in the case of the normal incidence of radiation on the cylinder axis). Calculations for an obliquely oriented cylinder were carried out in [17]. Within the limits of small particles, such as x, $|N|x \ll 1$ (where $x = ka$ is a wave or diffraction parameter; $k = 2\pi/\lambda$ is a wave number, $N = (n_2 + i\kappa_2)/(n_1 + i\kappa_1)$ is a complex index for refraction of the particle material with respect to the surrounding medium, i.e. air), we have

$$\text{cylinder:} \quad Q_{\mathrm{abs}} = \frac{\pi x}{4} \mathrm{Re}\left\{ -i(N^2 - 1)\frac{N^2 + 3}{N^2 + 1} \right\};$$
$$\alpha = \frac{2Q_{\mathrm{abs}}}{\pi a} = \alpha_{\mathrm{i}} \left[\frac{n_{\mathrm{i}}}{2} + \frac{2n_{\mathrm{i}}}{\left(1 + n_{\mathrm{i}}^2 - \kappa_{\mathrm{i}}^2\right)^2 + 4 n_{\mathrm{i}}^2 \kappa_{\mathrm{i}}^2} \right]$$

$$\text{sphere:} \quad Q_{\mathrm{abs}} = 4\mathrm{Im}\left\{ \frac{N^2 - 1}{N^2 + 2} \right\};$$
$$\alpha = \frac{3Q_{\mathrm{abs}}}{4a} = \alpha_{\mathrm{i}} \left[\frac{9 n_{\mathrm{i}}}{\left(n_{\mathrm{i}}^2 - \kappa_{\mathrm{i}}^2 + 2\right) + 4 n_{\mathrm{i}} \kappa_i} \right]. \tag{18}$$

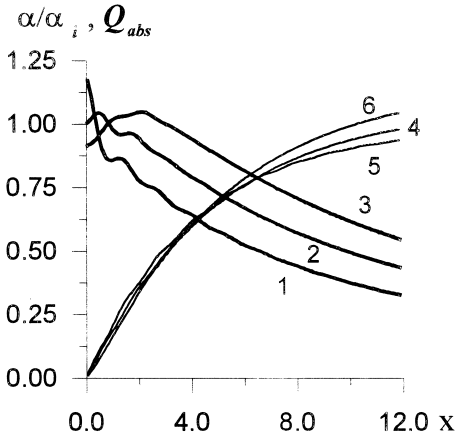

Fig. 1. Average volumetric absorption coefficient α (curves 1, 2, 3) and absorption factor Q_{abs} (4, 5, 6) as a function of diffraction parameter $x = ka$. 1 and 4 correspond to disk (infinite plate); 2, 5 to infinite cylinder; 3, 6 to sphere. Normal incident radiation, angle $\theta_1 = 0$.

We took into account that for air $N = n_1 \equiv 1$, $\kappa_1 = 0$. An absorption factor of an ice particle averaged over volume within the limits of small radii tends to $1.18\alpha_i$; $1.003\alpha_i$ and $0.915\alpha_i$ for the case of plate, cylinder and sphere, respectively. The α and Q_{abs} rigorous relations to the particle size a (to the diffraction parameter $x = ka$) are presented in Fig. 1, their relations to angle θ_1, in Fig. 2 In the case of oblique cylinder, the $\cos\theta_1$ law is a good approximation for the absorption coefficient α dependent on θ_1.

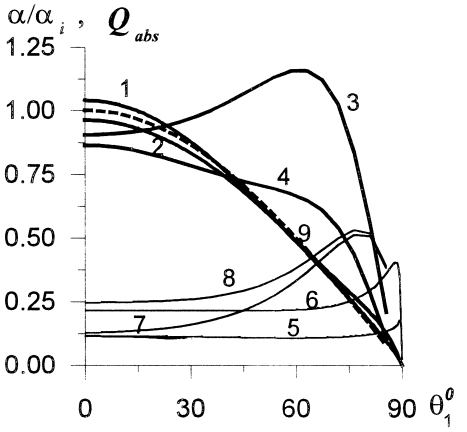

Fig. 2. Average volumetric absorption coefficients α (curves 1, 2, 3, 4) and absorption factors Q_{abs} (5, 6, 7, 8) versus incident angle θ_1. 1 and 5 correspond to infinite cylinder, radius $a = 1$ μm; 2, 6: infinite cylinder, $a = 2$ μm; 3, 7: infinite plate, thickness $h = 2a = 2$ μm; 4, 8: infinite plate, $2a = 4$ μm. Curve 9 (dashed line) is $\cos\theta_1$.

4. Heating and sublimation of particles

Integrating (13) with respect to the coordinate, for temperature T_{av} averaged over the particle volume, we get an equation with the initial condition:

$$\rho_i C_{pi}\frac{dT_{av}}{dt} = q - \frac{m+1}{a}(jH_i + j_T);$$
$$T_{av} = \frac{m+1}{a^{m+1}}\int_0^a Tr^m dr; \qquad (19)$$
$$m = 0, 1, 2;\ T_{av}|_{t=0} = T_\infty$$

Density, specific heat capacity and thermal conductivity of ice are equal to $\rho_i = 900$ kg/m^3, $C_{pi} = 2106$ J/kg, $\lambda_i = 2.20$ W/(m K) at a temperature of 273 K. Temperature-dependent on specific heat at constant pressure C_p, i, w, v for ice, water and vapor (at saturation line), latent evaporation heat $H_{i,w}$ and saturated vapor pressure $p_{si,w}$ over the ice and water surface, as well as diffusivity of vapor D in air and thermal conductivity of air λ are presented in Table 1 [4,5,18–20].

As a result of heating, the particle temperature quickly reaches a certain maximum value T_{max}, then slowly falls as the heat losses per unit volume increase while the particle size reduces. If the heat release intensity is insufficient, the temperature will never reach the melting one: $T_{max} < T_{melt} = 273$ K. A slow particle sublimation occurs. Let us define an upper threshold of *sublimation* regime or a lower threshold of *melting* regime with respect to the heat release intensity $q_{sub} = \alpha I_{0sub}$ from Eq. (19), when the temperature reaches its maximum $dT_{av}/dt = 0$ provided this maximum is equal to the melting temperature:

$$q_{sub} = \frac{m+1}{a}(jH_i + j_T)\big|_{T=T_{melt}}$$
$$\approx \frac{m+1}{ar_{ef}}\left\{\frac{\mu_v H_i\langle\rho D\rangle}{\mu p_\infty}\left[p_s(T_{melt}) - p_s(T_\infty)\right]\right. \qquad (20)$$
$$\left. + \lambda(T_{melt} - T_\infty)\right\}$$

Relations of *sublimation* (*melting*) thresholds q_{sub} to the ambient air temperature T_∞ are presented in Table 2 for plate ($m = 0$), cylinder ($m = 1$) and sphere ($m = 2$) in the case of the equal initial size $a_{pl} = a_{cyl} = a_{sph} = 1$ μm (see columns 2, 3, 4; radius of disk $L_{pl} = 10a_{pl}$, length of cylinder $L_{cyl} = 20a_{cyl}$) and in the case of the equal initial mass $m_0 = 2a_{pl}\pi L_{pl}^2\rho_i = \pi a_{cyl}^2 L_{cyl}\rho_i = 4\pi a_{sph}^3\rho_i/3 = 5.654 \times 10^{-10}$ g ($a_{pl} = 1$ μm, $m = 0$) for cylinder and sphere ($a_{cyl} = 2.154$ μm, $m = 1$; $a_{sph} = 5.313$ μm, $m = 2$; columns 5 and 6, correspondingly). Pressure p_∞ is equal to 1 bar (height equals 0 km). The sublimation threshold weakly

Table 1
Thermal physical and thermodynamic properties of ice, water, vapor and air

T (K)	C_p (kJ/kgK)		H (MJ/kg)		p_s (N/m^2)		D (10^{-5} m^2/s)	λ_a (W/m K)
	ice	water	i	w	i	w		air
203	1.60	4.40	2.84	2.68	0.261	0.524	1.30	0.0188
213	1.67	4.39	2.84	2.66	1.08	1.96	1.42	0.0196
223	1.75	4.38	2.839	2.63	3.93	6.35	1.55	0.0206
233	1.813	4.37	2.839	2.60	12.8	18.9	1.69	0.0213
243	1.870	4.36	2.839	2.58	38.0	50.9	1.88	0.0220
253	1.959	4.35	2.838	2.55	103	125	1.95	0.0228
263	2.031	4.27	2.837	2.52	260	286	2.08	0.0235
273	2.106	4.218	2.835	2.50	611	611	2.22	0.0241
283		4.193		2.477		1227.	2.36	0.0248
293		4.182		2.454		2337.	2.50	0.0255
303		4.179		2.430		4241.	2.65	0.0262
313		4.179		2.406		7375.	2.80	0.0271
323		4.181		2.383		12335.	3.00	0.0277
333		4.185		2.358		19917.	3.24	0.0285
343		4.190		2.338		31170.	3.40	0.0292
353		4.197		2.308		47360.	3.60	0.0299
363		4.205		2.282		70110.	3.80	0.0307
	vapor							
373	2.034	4.216		2.257		101325.	3.98	0.0314
393	2.100	4.245		2.202		1.99×10^5	4.38	0.0328
423	2.320	4.310		2.114		4.76...	4.70	0.0328
473	2.883	4.497		1.941		15.55...	6.12	0.0347
523	3.918	4.870		1.715		37.98...	7.34	0.0385
573	6.140	5.770		1.404		85.92...	8.66	0.0420
623	15.95	10.08		0.894		165.4...	10.0	0.0447
647	6198.	3087.		0.0		221.2×10^5	10.7	0.0487

depends on height. The lower line shows values of the averaged absorption coefficient α/α_i for conversion of the sublimation heat release intensity q_{sub} into the laser beam intensity $I_{0,\,sub} = q_{sub}/\alpha$.

Let us define the evaporation parameter $\beta = jH_i/(jH_i + j_T)$ as the portion of the full heat losses energy that is spent on evaporation and the evaporation efficiency $b = jH_i\,(m+1)/aq$ as the portion of the total energy absorbed by a particle that is spent on evaporation. Usually, the theory of water aerosol clearing does not draw a distinction between these values, since it is expected that droplet evaporation occurs in the regime of constant temperature, which is close to the maximum temperature.

At the sublimation (melting) threshold $dT_{av}/dt = 0$, these values coincide and are equal to

Table 2
Values of heat release intensity q_{sub}, W/m^3 at the boundary "sublimation–melting"

Temperature	Radii $a_{pl} = a_{cyl} = a_{sph} = 1$ (μm)			Mass $m_0 = 5.654 \times 10^{-10}$ g = *const*	
T (K)	$m = 0$	$m = 1$	$m = 2$	$m = 1$	$m = 2$
203	1.32×10^{11}	1.13×10^{12}	5.96×10^{12}	2.43×10^{11}	2.11×10^{11}
213	1.16×10^{11}	9.92×10^{11}	5.24×10^{12}	2.14×10^{11}	1.86×10^{11}
223	1.00×10^{11}	8.55×10^{11}	4.51×10^{12}	1.84×10^{11}	1.60×10^{11}
233	8.40×10^{10}	7.16×10^{11}	3.78×10^{12}	1.54×10^{11}	1.34×10^{11}
243	6.71×10^{10}	5.72×10^{11}	3.02×10^{12}	1.23×10^{11}	1.07×10^{11}
253	4.90×10^{10}	4.17×10^{11}	2.20×10^{12}	8.99×10^{10}	7.81×10^{10}
263	2.77×10^{10}	2.36×10^{11}	1.25×10^{12}	5.09×10^{10}	4.42×10^{10}
α/α_i	0.904	1.04	0.970	0.959	0.994

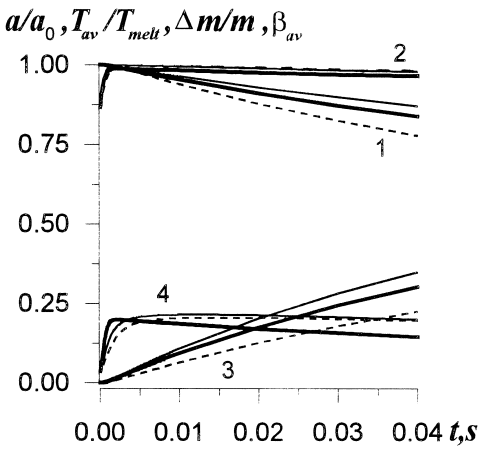

Fig. 3. (Initial interval). Time-dependent relative size of an ice aerosol particle a/a_0 (curves 1), average temperature $T_{\rm av}/T_{\rm melt}$ (curve 2), relative loss of mass $\Delta m/m_0$ (curve 3) in the sublimation regime and time-averaged evaporation parameter $\beta_{\rm av}$ (curve 4), for a disk of thickness $2a_{\rm pl} = 2$ μm and radius $L_{\rm pl} = 10$ μm (solid curves); for a cylinder of radius $a_{\rm cyl} = 2.154$ μm, and length $L_{\rm cyl} = 43.08$ μm (bold solid curves); for a sphere of radius $a_{\rm sph} = 5.313$ μm (dashed lines).

$$\beta = \left.\frac{jH_{\rm i}}{jH_{\rm i} + j_T}\right|_{T=T_{\max}} \approx \frac{1}{1 + \dfrac{\mu p_\infty \lambda (T_{\rm melt} - T_\infty)}{\mu_{\rm v} H_{\rm i} \langle \rho D \rangle \left[p_{\rm s}(T_{\rm melt}) - p_{\rm s}(T_\infty)\right]}} \approx b = \frac{(m+1) j H_{\rm i}}{aq} \tag{21}$$

In Figs. 3 and 4 (Fig. 3 is the initial interval, Fig. 4 is the whole interval), we plotted as a function of time relative size a/a_0 (curves 1), averaged particle temperature $T_{\rm av}(t)/273$ K (curves 2), relative loss of mass $\Delta m/m_0 = [m(t) - m_0]/m_0$ (curves 3) and average evaporation parameter $\beta_{\rm av} = [\int_0^t \beta \, {\rm d}t]/t$ (curves 4) for the disk with the initial thickness of $2a_{\rm pl} = 2$ μm and radius $L_{\rm pl} = 10a_{\rm pl} = 10$ μm for $q = 8.25 \times 10^{10}$ W/m^3 (solid curves); for the cylinder of radius $a_{\rm cyl} = 2.154$ μm and length $L_{\rm cyl} = 20a_{\rm cyl} = 43.08$ μm (bold solid curves) and for the sphere of radius $a_{\rm sph} = 5.313$ μm (dashed lines) at $q = 1.34 \times 10^{11}$ W/m^3. Temperature and pressure of air are equal to $T_\infty = 233$ K, $p_\infty = 1$ bar. The losses of mass and the average evaporation parameter are by the moment of time of 1 s for ice plate, cylinder and sphere $\Delta m/m_0 = 89$, 95 and 97%, $\beta_{\rm av} = 0.070$; 0.058 and 0.068, respectively.

The part of full heat losses energy spent on evaporation does not exceed $\beta_{\max} = 0.22$, 0.20, 0.23. Evaporation efficiency b is slightly different from the evaporation parameter β (b is slightly less than β on heating and is a little greater than β when the particle is cooling down).

The maximum particle temperature is equal to $(T_{\rm av})_{\max} = 272.9$; 264.2 and 272.9 K for the plate (disk), cylinder and sphere, respectively.

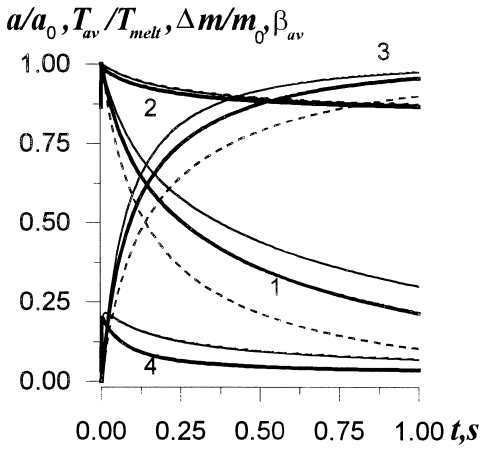

Fig. 4. Entire time interval.

5. Melting of particles

Energy consumption on melting a particle is equal to $E_{\rm melt} = \rho_{\rm i} H_{\rm melt} V_0$, where $H_{\rm melt} = 3.34 \times 10^5$ J/kg is specific heat of ice melting and V_0 is initial particle volume. We will consider the process of cylinder melting with some assumptions. Initial temperature is constant and equals the temperature of surrounding air. The temperature distribution is cylindrically symmetrical and the front of melting begins moving from the external surface inwards.

This situation is possible if at the initial moment the surface is covered by a thin water layer, which absorbs radiation better than ice, although the difference is rather small: $\alpha_{\rm w} = 8.18 \times 10^4$ m^{-1} > $\alpha_{\rm i} = 7.14 \times 10^4$ m^{-1}. Due to the heat losses from the surface, in this case the melting time of a particle will not reduce if the melting front moves from the center to the edge. For the plate (disk), there is no difference if the melting process begins with the surface exposed to radiation or with the opposite side. The latter is possible, since the distributed heat source for a plate 1–2 μm thick has a maximum on the surface that is opposite to the irradiated one [13].

The particle melting process is described by a one-dimension equation of heat conduction for water with the following boundary and initial conditions:

$$\rho_w C_{pw}\frac{\partial T}{\partial t}=\frac{1}{r^m}\frac{\partial}{\partial r}\left(r^m\lambda_w\frac{\partial T}{\partial r}\right)+q_w;\quad a\le r\le\zeta(t);\ m=0,1,2 \tag{22}$$

$$T|_{z=\xi(t)}=T_{melt}\equiv 273\ K;\quad T|_{t=0}=T_{melt};\quad \zeta(0)=\begin{cases}h=2a, & m=0\\ a, & m=1,2\end{cases} \tag{23}$$

$$-\lambda_w\frac{\partial T}{\partial r}\bigg|_{r=a}=(jH_w+j_T)\big|_{T_s=T(r=a)}\equiv J_w(T_s) \tag{24}$$

$$\lambda_w\frac{\partial T}{\partial r}\bigg|_{r=\zeta(t)}=\lambda_i\frac{\partial T}{\partial r}\bigg|_{r=\zeta(t)}-\rho_i H_{melt}\frac{d\zeta}{dt} \tag{25}$$

$$\lambda_i\frac{\partial T}{\partial r}\bigg|_{r=\zeta}=-q_i\frac{\zeta(t)}{m+1} \tag{26}$$

Here $\xi(t)$ is a coordinate of the moving front of the melted material (water); $q_i\equiv q$, $q_w=(\alpha_w/\alpha_i)q_i=1.146q_i$ is the average volumetric heat release intensity both, in solid and liquid phases. Ice temperature is close to the melting one, but during the melting process it remains less than T_{melt}. In the process of melting on the boundary of the melted material (water) at $r=\zeta(t)$, there is a sink of heat, which prevents the further heating of ice, until it melts down to water. Condition (26) is an integral of ice heating equation (13) for volume, under the condition $dT/dt\approx 0$. For the numerical solution of the problem, an implicit absolutely steady finite-difference scheme was applied using a run-procedure. For every time step Δt, the propagation step $\Delta\zeta$ and the propagation rate $d\zeta/dt=\Delta\zeta/\Delta t$ of the melting front (water front inside ice) were determined by means of an iterative algorithm. Temperature-dependent specific heat capacity, latent evaporation heat, water heat conductivity coefficient, and saturated vapour pressure over water, were taken from the tables with a step of 5 K.

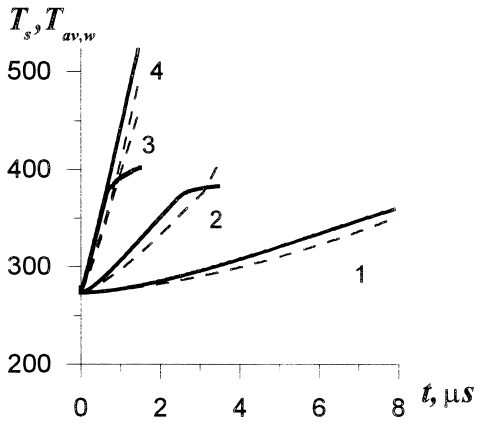

Fig. 5. Time-dependent cylinder surface temperature T_s and average volumetric temperature of water $T_{av,w}$ (dashed lines) at heat release intensities $q=7.20\times10^{13}$ (curves 1); 2.16×10^{14} (curves 2); 7.20×10^{14} W/m^3 (curve 3: taking into account surface evaporation, curve 4: without taking it into account, $J_w(T_s)=0$). Ambient air temperature is $T_\infty=233$ K, pressure $p_\infty=1$ bar, cylinder radius $a=2.154$ μm, length $L=43.08$ μm.

Fig. 5 shows time-dependent average water temperature T_{av}, $w=\int_{V(\zeta)}^{V_0}T\,dV/(V_0-V)$ (dotted lines) and surface temperature T_s for a cylinder of radius $a_{cyl}=2.154$ μm at a heat release intensity $q=7.20\times10^{13}$ (curve 1), 2.16×10^{14} (curve 2), 7.20×10^{14} W/m^3 (curve 3: with, and curve 4: without regard to the evaporation from the surface, $J_w(T_s)=0$). Here, $V_0=V(\zeta=a)$, $V(\zeta)$ is the initial and the current volume of ice in the particle, which equals $V(\zeta)=2\zeta\pi L^2$; $\pi\zeta^2L$; $4\pi\zeta^3/3$ for the disk, cylinder and sphere, accordingly; V_0-V is the volume of the melted material (water). The temperature of air is equal to $T_\infty=233$ K, the pressure equals $p_\infty\approx1$ bar. The account of evaporation has a noticeable influence on temperature distribution, but a weak influence on the total time of particle melting. The difference is less than 20%.

The melting time is $t_{melt}=413$, 49.2, 7.879 and 1.493 μs for $q\equiv q_i=7.20\times10^{11}$, 7.20×10^{12}, 7.20×10^{13}, 7.20×10^{14} W/m^3, respectively.

Values of the evaporation parameter averaged over the melting time are $\beta_{av}=0.212$, 0.228, 0.410, 0.739.

Values of the average temperature of the particle after melting are $T_{av}=279$, 294.1, 350, 463.8 K at $q=7.20\times10^{11}$, 7.20×10^{12}, 7.20×10^{13}, 7.20×10^{14} W/m^3. This temperature should be taken as initial when studying the evaporation process of the formed droplet. The velocity of the melting material front is $d\zeta/dt=0.0215$, 0.133, 0.547, and 2.217 m/s.

Losses of mass are insignificant and do not exceed 1% for the case of the most intensive heat release $q=7.20\times10^{14}$ W/m^3 of all the variants considered above.

As follows from equations of heating, melting and evaporation of particle (13), (19), (22)–(26), the least amount of energy is required for the particle heating, then for melting and finally, for evaporation, because of the fact that $C_p\Delta T<H_{melt}<H_i$, H_w. Respectively, the heating time is essentially shorter than the melting one, and the latter is substantially less than the evaporation time of the formed droplet.

We shall derive approximate expressions for the melting time t_{melt} using the results of the numerical calculation, according to which we have $dT_{av,w}/dt\approx\text{const}=K$, or $T_{av,w}\approx T_{melt}+tK$. Let us integrate Eq. (22) over the volume of water $\int_{V(\zeta)}^{V_0}\cdots dV$.

Using two auxiliary correlations

$$\frac{\mathrm{d}}{\mathrm{d}t}\left[T_{\mathrm{av,\,w}}(V_0-V)\right]=(V_0-V)\frac{\mathrm{d}T_{\mathrm{av,\,w}}}{\mathrm{d}t}-T_{\mathrm{av,\,w}}\frac{\mathrm{d}V}{\mathrm{d}t}$$
$$=K(V_0-V)-(T_{\mathrm{melt}}+Kt)\frac{\mathrm{d}V}{\mathrm{d}t}$$

$$\frac{\mathrm{d}}{\mathrm{d}t}\left[T_{\mathrm{av,\,w}}(V_0-V)\right]\equiv\frac{\partial}{\partial t}\left(\int_V^{V_0}T\,\mathrm{d}V\right)$$
$$=\int_V^{V_0}\frac{\partial T}{\partial t}\,\mathrm{d}V-T_{\mathrm{melt}}\frac{\mathrm{d}V}{\mathrm{d}t}$$

we derive for the left part of Eq. (22), the following expression

$$\rho_{\mathrm{w}}C_{\mathrm{pw}}\int_V^{V_0}\frac{\partial T}{\partial t}\,\mathrm{d}V=\rho_{\mathrm{w}}C_{\mathrm{pw}}K\left[V_0-V-t\frac{\mathrm{d}V}{\mathrm{d}t}\right].$$

Here we took into account the fact that on the melting material front, the temperature is equal to the melting temperature. In the right part of Eq. (22), the integration for water volume using the boundary conditions on the melting front on the water side (25) and the ice side (26) gives:

$$\int_V^{V_0}q_{\mathrm{w}}\,\mathrm{d}V+\int_V^{V_0}\frac{1}{r^m}\frac{\partial}{\partial r}\left(r^m\lambda_{\mathrm{w}}\frac{\partial T}{\partial r}\right)\mathrm{d}V$$
$$=q_{\mathrm{w}}(V_0-V)+S(r)\lambda_{\mathrm{w}}\frac{\partial T}{\partial r}\Big|_{\zeta}^{\zeta_0}$$
$$=q_{\mathrm{w}}(V_0-V)+\rho_{\mathrm{i}}H_{\mathrm{melt}}\frac{\mathrm{d}V}{\mathrm{d}t}+q_{\mathrm{i}}V-S_0J_{\mathrm{w}};$$
$$\zeta_0=\begin{cases}h=2a, & m=0\\ a, & m=1,2\end{cases},$$

where $S_0=\pi L_{\mathrm{pl}}^2$, $2\pi L_{\mathrm{cyl}}a_{\mathrm{cyl}}$, $4\pi a_{\mathrm{sph}}^2$ is the area of the external surface of a particle; $S(\zeta)=\pi L_{\mathrm{pl}}^2$, $2\pi L_{\mathrm{cyl}}\zeta$, $4\pi\zeta^2$ is the area of the melting material front surface for a disk, a cylinder and a sphere, respectively. We take into account the relationship $S(\zeta)\,\mathrm{d}\zeta/\mathrm{d}t=\mathrm{d}V/\mathrm{d}t$. Further, we neglect the heat and mass losses from the particle surfaces: $J_{\mathrm{w}}=0$. Approximate equations of particle melting and its solution have the form

$$\frac{\mathrm{d}V}{\mathrm{d}t}(\rho_{\mathrm{i}}H_{\mathrm{melt}}+K_1t)=V(q_{\mathrm{w}}-q_{\mathrm{i}}-K_1)-V_0(q_{\mathrm{w}}-K_1);$$
$$K_1=\rho_{\mathrm{w}}C_{\mathrm{pw}}K$$

$$t=\frac{\rho_{\mathrm{i}}H_{\mathrm{melt}}}{K_1}\left\{-1+\left[\frac{q_{\mathrm{w}}-K_1}{q_{\mathrm{i}}}\left(1-\frac{V}{V_0}\right)-\frac{V}{V_0}\right]^{\{K_1\}/\{q_{\mathrm{w}}-q_{\mathrm{i}}-K_1\}}\right\}$$

$$\frac{V(t)}{V_0}=1-\frac{q_{\mathrm{i}}}{q_{\mathrm{w}}-q_{\mathrm{i}}-K_1}\times\left[\left(1+\frac{tK_1}{\rho_{\mathrm{i}}H_{\mathrm{melt}}}\right)^{\{q_{\mathrm{w}}-q_{\mathrm{i}}\}/\{K_1\}-1}-1\right]\quad(27)$$

Hence it follows that, the melting time t_{melt} (at $V(\zeta=0)=0$) equals

$$t_{\mathrm{melt}}=\frac{\rho_{\mathrm{i}}H_{\mathrm{melt}}}{K_1}\left\{-1+\left[\frac{q_w-K_1}{q_{\mathrm{i}}}\right]^{\{K_1\}/\{q_{\mathrm{w}}-q_{\mathrm{i}}-K_1\}}\right\}\quad(28)$$

Using the results of the numerical solution of the melting problem, we will take $K=1.32\times10^4$, 4.29×10^5, 9.77×10^6, 1.28×10^8 K/s at $q_{\mathrm{i}}=7.20\times10^{11}$, 7.20×10^{12}, 7.20×10^{13}, 7.20×10^{14} W/m^3. In Fig. 6, the following results for an ice cylinder are presented: exact dependence $t_{\mathrm{melt}}(q_{\mathrm{i}})$ (curve 1), an approximate dependence calculated using formula (28) (curve 2), and sim-

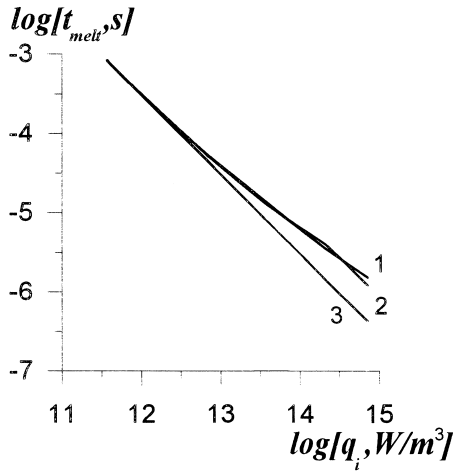

Fig. 6. Melting time t_{melt} relations to heat release intensity q_{i}: 1 is an exact solution; 2 is an approximate formula (28); 3 is the simplest approximation $t_{\mathrm{melt}}(q_{\mathrm{i}})=\rho_{\mathrm{i}}H_{\mathrm{melt}}/q_{\mathrm{i}}$.

plest approximation of the relationship between the ice particle melting time and the intensity of heat release q_i:$t_{melt}(q_i) = \rho_i H_{melt}/q_i$ (curve 3), which directly expresses the energy conservation law if we multiply the numerator and the denominator by the particle volume. The inaccuracy of formula (28) is less than 3% at $q_i \le 7.2 \times 10^{12}$ W/m^3 and does not exceed 19.8% at $q_i \le 7.20 \times 10^{14}$ W/m^3.

The similar comparison of approximate expression (28) with the exact melting time of a plate (disk) shows that inaccuracy does not exceed 4.0% at $q_i \le 3.20 \times 10^{14}$ W/m^3. The numerical constants K for the plate having the same mass as the cylinder, i.e. at $a_{pl} = 1$ μm, $L_{pl} = 10$ μm are: $K = 3.292 \times 10^3$, 2.268×10^5, 6.95×10^6, 4.778×10^7 K/s at $q_i = 6.4 \times 10^{11}$, 6.4×10^{12}, 6.4×10^{13}, 3.2×10^{14} W/m^3.

Both the considered approximations, the simplest one and the one derived from formula (28), depend on the form of the particle through the intensity of heat release $q = \alpha I_0$, i.e. through the average volumetric coefficient of radiation absorption α. This quantity is important in the nonlinear optics of aerosols. The form of the particles also affects the temperature increase rate K. And, finally, the value of heat losses from the particle surface due to evaporation J_w, which for particles of equal mass increases when passing from the plate to the cylinder, and from the cylinder to the sphere, can be a reason of inconstancy of value K and difference between the approximate value t_{melt} and the exact one.

The influence of variation in temperature T_∞ and pressure p_∞ of the surrounding air on the melting process is small.

6. Evaporation of the formed droplet

The process of droplet evaporation at the approximation of uniform heat release and uniform temperature field inside the droplet is described by Eqs. (19) and (14), in which physical parameters of water are used. The radius of the formed droplet ($a_{sph} = 5.130$ μm) is smaller than that of the ice sphere of the equal mass, which is 5.313 μm due to the lower ice density in comparison with that of water.

The calculations of all stages of particle destruction (heating, melting, sublimation and evaporation) were carried out for a cylinder of initial radius $a_{cyl} = 2.154$ μm at an air temperature $T_\infty = 203$–233 K and a pressure $p_\infty = 1$–0.55 bar (height 0–20 km), within the range of heat release intensity from the upper threshold of sublimation (lower threshold of melting) $q_i = 1.84 \times 10^{11}$ W/m^3 up to $q_i = 7.2 \times 10^{14}$ W/m^3.

In Table 3, the following values are presented as a function of radiation intensity I_0: heating time t_{heat} up to 273 K, melting time t_{melt} (including t_{heat}) and evaporation time t_{vap} (including t_{melt}) up to the moment when the particle loses 95% of mass; the values of evaporation parameter β_{av} and evaporation efficiency $b_{av} = [\int_0^t b\, dt]/t$ averaged over time; maximum temperature $T_{av,\,max}$ and volumetric averaged temperature T_{av} at the end of the evaporation process. The physical parameters of a spherical supercooled water droplet of equal mass are presented in the lower lines of some cells of the table. Air temperature is $T_\infty = 233$ K, pressure is $p_\infty = 1$ bar (height equals 0 km).

Temperatures averaged over volume for the cylinder and the sphere are identical, both, when the maximum

Table 3
Heating time t_{heat}, melting time t_{melt}, evaporation time t_{vap}, evaporation parameter β_{av} and evaporation efficiency b_{av} of ice cylinder, maximum temperature $T_{av,\,max}$ and temperature at the end of the evaporation process T_{av} up to 95% loss of mass. Initial cylinder radius is $a_{cyl} = 2.154$ μm, cylinder length is $L_{cyl} = 43.08$ μm, air temperature is $T_\infty = 233$ K, air pressure is $p_\infty = 1$ bar. The lower line in each cell gives values for a supercooled water droplet of equivalent mass (radius is $a_{sph} = 5.130$ μm)

$I0$ (MW/m^2)	$t$heat (μs)	$t$melt (μs)	$t$vap (ms)	$b$av	βav	Tav, max (K)	Tav (K)
5	265.	1030.	95.43	0.122	0.194	298.2	252.3
			94.80	0.122	0.195	298.6	252.4
10	115.	601.5	27.64	0.207	0.331	314.7	266.4
			27.36	0.209	0.332	314.8	266.4
50	21.0	117.9	2.72	0.406	0.655	347.4	307.5
			2.66	0.414	0.664	347.5	307.4
100	10.4	62.56	1.23	0.442	0.709	358.8	323.1
			1.20	0.453	0.732	358.8	323.0
500	2.10	15.97	0.229	0.523	0.824	378.1	354.1
			0.223	0.537	0.835	378.1	354.1
1000	1.03	9.278	0.0987	0.837	0.952	384.4	374.9
			0.0956	0.866	0.966	384.4	374.9
5000	0.206	2.811	0.0182	0.893	0.966	420.6	392.3
			0.0174	0.930	0.979	419.7	392.5

is achieved and when the mass is reduced by 95%. The total evaporation time, time-averaged evaporation parameter β_{av} and evaporation efficiency b_{av} are different by a few percent only.

Due to the small energy expenditure on particles heating and melting and the slight difference between thermal physical and optical characteristics of ice and water, in the first place, coefficients of radiation absorption and latent heat of evaporation, the difference in the characteristics of the evaporation process of an ice cylinder (as well as a plates or a disk) and a water droplet is small. Time of evaporation is different by not more than 4.4% within the range of radiation intensities $I_0 = 5 \times 10^6$–5×10^9 W/m^2. The essential distinction is between the evaporation characteristics of the droplet and the cylinder, the axis of which is situated at a small angle $\varphi = \pi/2 - \theta_1$ with the parallel radiation beam. In the limiting case, the base of the cylinder is turned to the beam and receives minimum part of the radiation flow, which is equal to $\pi(a_{cyl})^2/2a_{cyl}L_{cyl} = \pi/40 = 0.0785$, compared with the case when the beam incidence is perpendicular to the cylinder axis. Figs. 7 and 8 presents the results for the case $\varphi = 5.73^\circ$ ($I_0 = 10^8$ W/m^2, $T_\infty = 233$ K; $p_\infty = 1$ bar; $a_{cyl} = 2.154$ μm, radius of the equivalent sphere is $a_{sph} = 5.130$ μm). In Fig. 7, the time dependence is shown for the temperature, the solid curve corresponds to the cylinder, the dotted line corresponds to the supercooled water droplet of equivalent mass. In Fig. 8, time dependence is presented for relative mass losses $\Delta m/m_0$, curve 1, time-averaged evaporation parameter β_{av} (curve 2) and evaporation efficiency b_{av} (curve 3). Dotted lines correspond to the respective relations for the supercooled water spherical droplet. Difference of evaporation time due to the increase in heating and melting time for the ice cylinder is 44.7%.

Reduction of air temperature, for instance down to 203 K, firstly, enlarges the temperature difference between the particle and the ambient air and increases the heat flow value j_T; secondly, enlarges concentration difference and vapor flow density j. For the cylinder, the time of evaporation is $t_{vap} = 80.61$, 1.282, 0.0992 ms at $I_0 = 10^7$; 10^8; 10^9 W/m^2. Average evaporation parameter β_{av} and evaporation efficiency b_{av} were equal to $b_{av} = 0.071$, 0.424, 0.833 and $\beta_{av} = 0.113$, 0.685, 0.942 by the moment of mass reduction by 95%. Maximum values of temperature equal to $T_{av,\,max} = 311.7$, 358.7, 384.4 K are reached at the time moments $t = 1.41$; 0.142; 0.0144 ms. Difference between evaporation features of a supercooled spherical droplet and an ice cylinder is insignificant. Difference between evaporation features of the cylinder at the air temperature $T_\infty = 203$ and 233 K is 192; 4.2; 0.5% for the evaporation time t_{vap}; 193; 3.4; 1.05% for the evaporation parameter β_{av} and 65.7; 4.1; 0.48% for the evaporation efficiency b_{av} at the radiation intensity $I_0 = 10^7$; 10^8; 10^9 W/m^2, respectively. The evaporation time in magnitude increases by 2.92 times, and the time-averaged evaporation efficiency decreases by 2.93 times. Therefore, at lower beam intensities the difference in evaporation features due to air cooling is essential, and it is necessary to take into account the influence of air temperature reduction in the problems of aerosol clearing.

Reduction of surrounding air pressure as the height grows $p_\infty = 0.5401$, 0.265, 0.121, 0.055 bar (height is 5, 10, 15, 20 km) results in reduction of the boiling

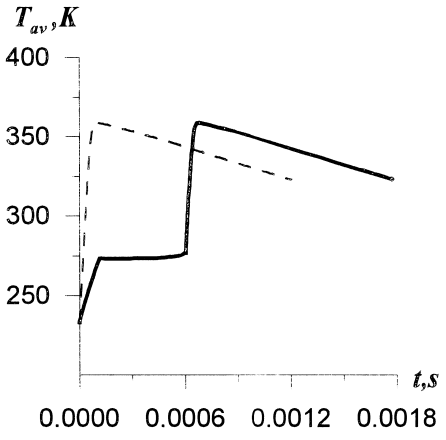

Fig. 7. Temperature of evaporating cylinder (solid curve, $a_{cyl} = 2.154$ μm) and supercooled droplet of equivalent mass (dashed line, $a_{sph} = 5.130$ μm). Beam intensity $I_0 = 10^8$ W/m^2, air temperature $T_\infty = 233$ K; pressure $p_\infty = 1$ bar; angle of beam deviation from the cylinder axis $\varphi = 5.73^\circ$.

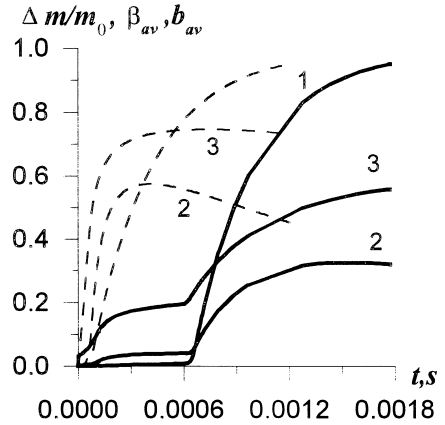

Fig. 8. Relative mass loss $\Delta m/m_0$ (curves 1), time-averaged evaporation parameter β_{av} (curves 2) and evaporation efficiency b_{av} (curves 3). Solid lines: cylinder, dashed lines: supercooled spherical droplet.

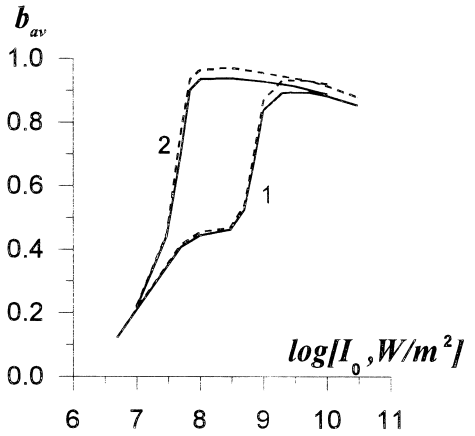

Fig. 9. Time-averaged evaporation efficiency b_{av} (at the moment of the 95% loss of mass) versus laser beam intensity I_0, W/m^2 for an ice cylinder and a supercooled spherical water droplet (dashed line) at a height of 0 km (curves 1, $p_\infty = 1$ bar) and 20 km (curves 2, $p_\infty = 0.055$ bar). Ambient air temperature $T_\infty = 233$ K.

temperature down to the values $T_b = 356.3$, 339.3, 322.8, 307.3 K and in reduction of the boundary temperature, which separates the diffusive and the gas dynamic regimes of evaporation. This temperature is close to the boiling temperature. For the same values of droplet surface temperature (radius equals 5 μm) $T_s = 307$, 311, 371, 381 K, the values of density of vapor flow $j(T_s)$ and density of heat loss flow from the surface $J(T_s) = jH_w + j_T$ are $j = 0.205$, 0.261, 13.0, 39.1 kg/m^2; $J = 0.937$, 1.113, 40.0, 86.7 MW/m^2 at a height of 0 km and $j = 0.70$, 1.50, 70.7, 99.1 kg/m^2; $J = 2.50$, 4.00, 157.2, 217.5 MW/m^2 at a height of 20 km. Heat and mass losses from the surface increase due to the transition from the diffusive regimes of evaporation to the gas dynamic ones at the lower values of temperature. The features of the evaporation process noticeably change in comparison with the case of pressure $p_\infty = 1$ bar in the wide range of intensity (see Table 4).

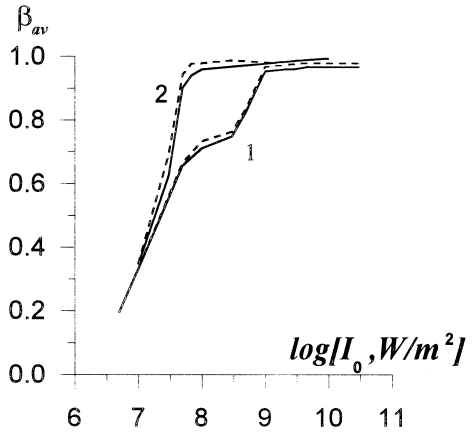

Fig. 10. Same as in Fig. 9 but for averaged evaporation parameter β_{av}.

In Fig. 9, the values of evaporation efficiency b_{av} depending on the laser beam intensity are shown at a height 0 km (curve 1) and 20 km (curve 2). Ambient air temperature is $T_\infty = 233$ K. In Fig. 10, the evaporation parameter is plotted versus the intensity I_0 at a height of 0 km (curve 1) and 20 km (curve 2) for the ice cylinder. Air temperature is the same $T_\infty = 233$ K. Dashed curves correspond to the evaporation of a supercooled spherical water droplet. The difference with respect to the characteristics of sphere evaporation is small.

Difference in evaporation features of the cylinder at heights of 0 and 20 km, namely, in values of evaporation parameter β_{av} and evaporation efficiency b_{av}, and also evaporation time t_{vap} is maximum at $I_0 = 10^8$ W/m^2 and is small at $I_0 < 10^7$ or $I_0 > 10^9$ W/m^2. The divergence is due to the reduction of the boiling temperature at great heights, as shown in Fig. 11 At $I_0 = 10^7$ W/m^2, the particle temperature falls to the water freezing temperature by the end of the evaporation process. The increased rate of the averaged volumetric temperature T_{av} falls at intensities $I_0 > 7 \times 10^7$ W/m^2 (at a height of 20 km) and $I_0 > 8 \times 10^8$ W/m^2 (at a height of 0 km) due to the excess of boiling temperature $T_b = 307.3$ and 373 K. Small reduction of the evaporation efficiency in the field of high values of

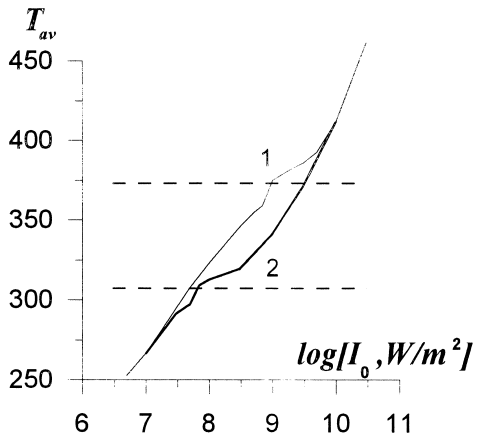

Fig. 11. Averaged temperature T_{av} K (at the moment of 95% loss of mass) vs. laser beam intensity I_0, W/m^2 for an ice cylinder and a supercooled spherical water droplet (dashed line) at height of 0 km (curves 1) and 20 km (curves 2). Dashed lines show the boiling temperature levels $T_b = 373$ K (0 km); 307.3 K (20 km). Ambient air temperature $T_\infty = 233$ K.

radiation intensity I_0 is due to the overheat of water (including the remaining 5% mass of the droplet) and the vapor that escapes the surface of the particle, i.e., after all, due to the overheat of the surrounding space. Maximum values of the evaporation efficiency correspond to the radiation intensity values equal to $I_0 \approx 10^8$ W/m^2 and 3×10^9 W/m^2 at heights of 20 and 0 km, for which the average volumetric temperature of the droplet slightly exceeds the boiling temperature.

The energy loss necessary for evaporation of particles decreases as the intensity grows (refer to the fifth column in Table 4). However, at the stage of heating up to the maximum temperature, the temperature gradient in the droplet is great and the *conditions of explosive destruction* can be achieved. For the droplet radius of $a = 1$–5.13 μm, the explosive intensity threshold is [21] $I_{\text{expl}} = Pe_{\text{expl}}\lambda T_{\text{crit}}/\alpha_{\text{w}}a^2 \approx 4.62 \times 10^9$–$1.76 \times 10^8$ W/m^2, where $Pe_{\text{expl}} = 1.13$–1.23 is the calculated Peclet number of explosion, λ (583 K) = 0.522 W/m K is the characteristic value of water heat conduction, $T_{\text{crit}} = 647.3$ K is the critical water temperature. Time of achieving the explosion conditions equals $t_{\text{expl}} = \rho_{\text{crit}}[h_{\text{expl}} - h_{\text{w0}}]/\alpha_{\text{w}}I_{\text{expl}} \approx 3.33 \times 10^{-5}$–$1.33 \times 10^{-6}$ s, where ρ_{crit} is the characteristic value of water density (here $\rho_{\text{crit}} = 317.76$ kg/m^3 is water density in the critical condition), h_{expl}, h_{w0} are water enthalpies at the moment of explosion and at the initial moment, respectively. Usually, the initial water enthalpy h_{w0} can be neglected. The explosive enthalpy h_{expl} is close to the value h_{s} along the line of absolute instability of water (spinodal). For the purpose of evaluation, we take that $h_{\text{expl}} \approx h_{\text{s}} \approx 1.6$ kJ/kg at the temperature of explosion $T_{\text{expl}} = 583$–603 K [22]. As to the order of magnitude, the time of reaching the explosive conditions is equal to the time of reaching the maximum temperature inside the droplet. After having exploded, the droplet disintegrates into several (3–4) smaller particles. The evaporation time for the latter ones will exceed the evaporation time of the initial droplet, since both the evaporation parameter and the evaporation efficiency decrease as the droplet size reduces. The total energy expenditure on evaporation can turn out to be greater than in the regular evaporation regime. A model for explosion of the droplet aerosol was considered for example in [23].

7. Conclusion

The paper states the basic stages for creation of an aerosol clearing theory including aerosols with ice particles. Conditions of heat and mass transfer from the surfaces for three classes of aerosol ice particles, which are disks (plates), cylinders and spheres, are different only in effective radii.

Thresholds of intensity for the sublimation regime (destruction without melting) are defined on the basis of averaged equations of energy and mass conservation inside particles, considering the boundary conditions of heat and mass transfer on the particle surface.

It is found that for the particles of micron radius it is possible to neglect the nonuniformity of temperature distribution inside the particle at the stage of heating up to the melting temperature. Particle melting is

Table 4
Maximum particle temperature $T_{\text{av, max}}$; time of reaching this temperature t_{max}; evaporation time t_{vap}; density of laser beam radiation energy at the moment of particle evaporation $E = I_0 t_{\text{vap}}$; evaporation efficiency b_{av} and evaporation parameter β_{av} for cylinder; average temperature T_{av} at the end of evaporation process up to 95% loss of mass. Initial cylinder radius is $a_{\text{cyl}} = 2.154$ μm, length is $L_{\text{cyl}} = 43.08$ μm, air temperature is $T_\infty = 233$ K, pressure is $p_\infty = 0.055$ bar (height is 20 km). The lower lines give values for a supercooled water droplet of equivalent mass (radius is $a_{\text{sph}} = 5.130$ μm)

I_0 (10 MW/m^2)	$T_{\text{av, max}}$ (K)	t_{max} (μs)	t_{vap} (ms)	E (J/cm^2)	b_{av}	β_{av}	T_{av} (K)
1	301.6	1369.	26.47	26.47	0.2154	0.3462	266.2
	302.3	640.	26.12	26.12	0.2196	0.3489	266.3
3	310.9	387.4	4.887	14.66	0.4419	0.6228	291.2
	310.9	330.0	4.830	14.49	0.4476	0.6894	291.1
10	318.0	98.6	0.951	9.51	0.9338	0.9574	312.4
	318.1	66.0	0.920	9.20	0.9631	0.9779	312.4
30	334.8	42.89	0.312	9.36	0.9360	0.9667	319.2
	334.8	33.0	0.303	9.09	0.9703	0.9873	319.2
100	365.2	16.1	0.0921	9.21	0.9253	0.9761	341.2
	365.4	12.6	0.0893	8.93	0.9529	0.9812	341.2
300	399.8	6.482	0.0301	9.03	0.9127	0.9845	370.8
	400.2	5.130	0.0292	8.49	0.9360	0.9854	370.9
1000	457.1	1.682	0.00865	8.65	0.8864	0.9916	412.0
	449.4	2.000	0.00850	8.50	0.9167	0.9918	411.8

characterized by low evaporation efficiency and comparatively small losses of the particle mass (for the maximum intensity of the considered intensity range, they are equal to several percent). At high values of intensity, the excess of the average temperature over the surface temperature is possible due to the overheated internal volume of the fluid phase.

Evaporation characteristics of a supercooled water droplet and an ice cylinder of equal mass are essentially different for the cylinders, the axes of which are at a small angle with the parallel flow of radiation.

For comparatively small radiation intensity, the reduction of ambient air temperature results in a significant reduction of the evaporation efficiency and an increase of evaporation time by several times. Pressure reduction of the surrounding air brings about an essential increase in the evaporation parameter and evaporation efficiency in the wide range of radiation intensity values due to the realization of gas dynamic regimes of evaporation at lower temperatures.

The difference in the evaporation process characteristics is caused firstly, by the difference in the geometric form of ice particles. Maximum differences occur between the plate (disk) and the sphere of equal mass, smaller differences exist between the cylinder (needle) and the plate or sphere.

Acknowledgements

Work was done under the financial support of International Scientific Technical Center (ISTC), project 200.

References

[1] H.C. van de Hulst, Light Scattering by Small Particles, Wiley, New York, 1957.
[2] D. Deirmendjian, Electromagnetic Scattering on Spherical Polydispersions, Elsevier, New York, 1969.
[3] C.F. Bohren, D.R. Huffman, Absorption and Scattering of Light by Small Particles, Wiley, New York, 1983.
[4] I.P. Mazin, S.M. Shmeter, Clouds, structure and creation physics, Gidrometeoizdat, Leningrad, 1983.
[5] I.P. Mazin, A.Kh. Khrgian (Eds.), Clouds and Cloudy Atmosphere, Handbook, Gidrometeoizdat, Leningrad, 1989.
[6] A.R. MacKenzie, M. Kulmala, A. Laaksonen, T. Vesala, On the theories of type I polar stratospheric clouds formation, Journal of Geophysical Research 100 (1995) 11275–11288.
[7] O.A. Volkovitsky, Yu.S. Sedunov, L.P. Semenov, Propagation of Intense Laser Radiation in Clouds, Gidrometeoizdat, Leningrad, 1982.
[8] A.P. Prishivalko, Optical and Heat Fields inside the Light Scattering Particles, Nauka i Tekhnika, Minsk, 1957.
[9] V.E. Zuev, A.A. Zemljanov, Yu.D. Kopytin, A.V. Kuzikovskii, High Power Laser Radiation in Atmospheric Aerosols, D. Reidel, Holland, 1985.
[10] E.V. Ivanov, V.Ya. Korovin, Experimental investigation of laser radiation $\lambda = 10.6$ μm impact on ice plates, Proceedings of the Institute of Experimental Meteorology (IEM) Obninsk Kaluga Region 5 (43) (1974) 115–132.
[11] V.Ya. Korovin, Acts of laser radiation $\lambda = 10.6$ μm on ice plate crystals, Proceedings of IEM Obninsk Kaluga region 11 (54) (1975) 34–40.
[12] P.N. Svirkunov, L.P. Semenov, Radiation interaction with ice crystals, Proceedings of IEM, Obninsk, Kaluga Region 5 (43) (1974) 5–30.
[13] P.N. Svirkunov, L.P. Semenov, Some questions of radiation interaction with droplets and ice crystals, Proceedings of IEM, Obninsk, Kaluga Region 11 (54) (1975) 3–18.
[14] J.O. Hirshfelder, Ch.F. Curtiss, R.B. Bird, Molecular Theory of Gases, Wiley, New York, 1954.
[15] W.W. Irvine, J.B. Pollack, Infrared optical properties of water and ice spheres, Icarus 8 (1968) 324–360.
[16] M. Born, E. Volf, Principles of Optics, Pergamon Press, Oxford, London, New York, Paris, Frankfurt, 1968.
[17] A.C. Lind, J.M. Greenberg, Electromagnetic scattering by obliquely oriented cylinders, Journal of Applied Physics 37 (1966) 3195–3203.
[18] J.E. Mc Donald, Saturation vapor pressure over supercooled water, Journal of Geophysical Research 70 (1965) 1553–1554.
[19] Tables of Physical Values. Handbook, I.K. Kikoin (Ed.), Àtomizdat, Moscow, 1976, 1006 pp.; Physical Values, I.S. Grigoriev, and Ye.Z. Meilikhov (Eds.), Energoatomizdat, Moscow, 1991, 1232 pp.
[20] A.A. Aleksandrov, M.P. Vukalovich, S.L. Rivkin, Tables of Thermal Physical Values of Water and Water Vapor, Izdatelstvo standartov, Moscow, 1969.
[21] A.N. Kucherov, Evaporation and explosion of overheated droplet in isobaric regimes, High Temperature 30 (1992) 761–767.
[22] V.P. Skripov, Ye.N. Sinitsin, P.A. Pavlov, G.V. Yermakov, G.N. Muratov, N.V. Bulanov, V.G. Baidakov, Thermophysics of Liquids in Metastable State, Àtomizdat, Moscow, 1980.
[23] V.P. Kandidov, M.S. Prakhov, Optical radiation propagation through a polydispersion water aerosol, Izvestiya AN SSSR. Physics of Atmosphere and Ocean 22 (1986) 265–273.